

Stochastic nature of the domain wall depinning in permalloy magnetic nanowiresJohanna Akerman,¹ Manuel Muñoz,² Marco Maicas,¹ and José L. Prieto¹¹*Instituto de Sistemas Optoelectrónicos y Microtecnología (ISOM), Universidad Politécnica de Madrid, Avda. Complutense s/n, 28040 Madrid, Spain*²*Instituto de Física Aplicada, CSIC, C/Serrano 144, 28006 Madrid, Spain*

(Received 28 July 2010; published 31 August 2010)

This study explores experimentally the stochastic nature of the domain wall depinning in permalloy nanowires using notches of various shapes and depths. The presence of the domain wall in the notch is detected through its anisotropic magnetoresistance (AMR), which is measured with high precision in order to detect even small changes in the domain wall profile. These measurements showed that variations in the depinning field are related with changes, sometimes very small, in the AMR profile, which indicates that small changes in the pinned domain wall profile can affect largely the depinning process. As these small changes are many times unpredictable and uncontrollable, the stochastic nature of the depinning could have negative consequences for practical applications based on permalloy nanowires.

DOI: [10.1103/PhysRevB.82.064426](https://doi.org/10.1103/PhysRevB.82.064426)

PACS number(s): 75.70.Kw, 75.75.-c, 75.78.Fg

Several of the next future magnetic technologies might rely on a careful and predictable control of magnetic domain walls (DWs) in ferromagnetic nanowires. The possibility of moving a DW or even achieving magnetic switching by means of spin-polarized currents¹ opens a great deal of potential applications. One of them is related to the development of future magnetic memories, where the bits move (rather than the disk like in the actual magnetic hard drives). The concept of the race-track memory was suggested by Stuart Parkin at IBM (Refs. 2 and 3) and it is based on storing the information on artificially created magnetic domains in a ferromagnetic nanowire. The magnetic DWs are pinned in artificially created notches along the wire and the distance between them constitute essentially the size of the bit unit. Despite the many potential advantages of this type of memory, its success is still pending on the reliable current depinning of a DW from an artificial notch.⁴ The idea of the race-track memory boosted recently the research on the interaction of a DW with an artificial notch, for different shapes (triangular or rectangular) or relative size with respect to the dimensions of the wire. It has been shown that the depinning field is higher for narrower wires⁵ and that the width of the wire is more relevant for the depinning than the geometry of the notch (for triangles and rectangles). The chirality of the DW also changes the depinning energy for asymmetric notches⁵⁻⁷ and increasing the depth of these notches would increase the pinning potential,⁸ unless they are too deep in which case they could induce double nucleation.⁹

Moreover, few works mention the stochastic behavior of the DW trapped in an artificial notch,¹⁰⁻¹² which is key for the development of any of the applications mentioned in the introduction. Very recently Im *et al.*¹³ studied by direct observation (x-ray microscopy) the stochastic behavior of DW trapped in triangular notches in permalloy wires of different widths. The measurements in this work showed considerable dispersion in the values of the depinning field and the authors concluded that this dispersion was presumably caused by the diversity of generable DW structures in the vicinity of a notch. Here we show evidence of this diversity of generable DW structures. Using a simple compensation method,

we have been able to measure accurately the anisotropic magnetoresistance (AMR) profile of the pinned DW and we have observed a direct relation between variations in the depinning field and changes in the AMR profile of the DW (i.e., a change in the DW structure). We have extended the study to several notch shapes, in a symmetrical configuration (on both sides of the wire) and performed a statistical study in different wires, showing that it is not possible to find a perfectly defined depinning field for any notch shape or depth. We have analyzed these results with micromagnetic simulations and we come to the conclusion that this stochastic nature of the DW pinning in permalloy nanowires might not be easily avoided. These results have a clear impact in the field, as artificial notches based on constrictions in the permalloy wire might not be the most reliable way to pin a DW. Research might have to focus in other type of defects, perhaps structural.¹⁴

The permalloy wires were fabricated by lift-off technique on $10 \times 5 \text{ mm}^2$ Si/SiO₂ substrates. The permalloy was deposited by dc magnetron sputtering with the structure Cr(1 nm)/NiFe(12 nm)/Au(1 nm). The film thickness was verified in an atomic force microscope where we also checked the good quality of the samples. The wire width is 500 nm in all the wires and two identical notches of different shapes were patterned on both sides of the wire with depths 75 and 125 nm (so the total constriction is 150 nm and 250 nm, respectively). From here on we will refer to the 75 nm dual notches as “shallow” and to the 125 nm dual notches as “deep.” The patterning was done by e-beam lithography (Crestec CABL9500) with the smallest beam current (10 pA) in order to shape the notches with the highest possible resolution. The results shown in this paper were obtained from two samples, one with wires with 75 nm deep notches (shallow) and another with wires with 125 nm deep notches (deep). Each sample contains at least seven wires with notches of each type. Other samples were used for confirmation purposes but the results are not shown here.

Figure 1 shows a scanning electron microscope (SEM) image of a nanowire with the Cr(1 nm)/Au(50 nm) contacts with a detail of a selected notch always located between contacts B and C. The wire has an injection elliptical pad in

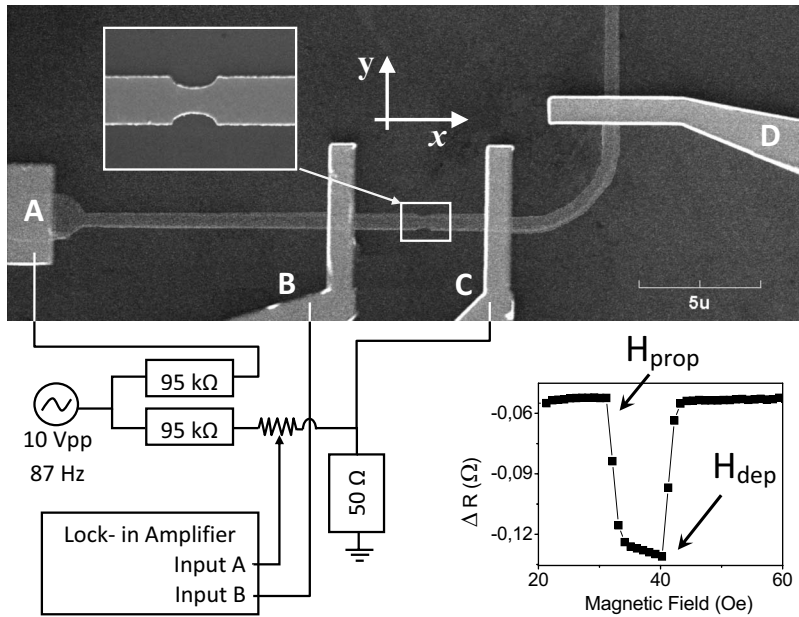


FIG. 1. SEM picture of one of the wires used for this study (top). Within the picture there is a zoom of the double notch in the wire. On the bottom left, there is a schematic of the setup used for the electrical detection of the domain wall through its associated decrease in the AMR in the section B-C. On the bottom right there is a selected graph with a pinning and depinning event measured by AMR. The first fall edge is taken as the propagation field and the second rise edge is the depinning field.

one extreme and a curved section at the opposite end. This curved section allows us to verify that when there is a depinning event, the DW shows up in the curved section (between contacts C and D) so we are certain we are measuring a DW and not other type of spurious signal. Within the same picture there is a diagram of the connections used for the electrical detection of the DW. The DW is detected by the decrease in the electrical resistance that it produces (anisotropic magnetoresistance or AMR) with a lock-in technique. Due to the very small AMR signal introduced by a DW, we have placed a variable series resistance so we compensate the output voltage to zero prior the injection of the DW. This zero method allows us to measure very accurately the AMR signal introduced by the DW. The resistance of our permalloy wires is typically around 280Ω and the AMR jump introduced by the DW ranges from 60 to 110 m Ω .

The measurement procedure is as follows. For each type of notch we measure the propagation and the depinning field: we apply a saturating field (up to 2 kOe) along the $-x$ -axis direction and then we monitor the resistance between contacts B and C for the magnetization process in the $+x$ direction. The inset of Fig. 1 (bottom right) shows a selected AMR curve for an injected DW in which the first fall edge constitutes the propagation field (H_{prop}) and the rise edge is the depinning field (H_{dep}). Note that the injection field from the elliptical notch might not be the same as the propagation field. This procedure is repeated at least 40 times for each wire and measured for different wires with the same type of notch.

Figure 2 shows the values for H_{prop} and H_{dep} for shallow notches (top) and for deep notches (bottom). On top of the figure we show SEM images for the different types of notches: square (S), triangle (T), square-left (SL), square-right (SR), elliptical (E), and circular (C). Each point in Fig. 2 represents the average H_{prop} and H_{dep} values measured over 40 magnetization loops for a particular wire within the sample. The different points in a particular type of notch are values measured in different wires. In the cases with less

points represented (for instance, E shallow), we found only that number of wires where we could see pinning events (for instance, only one wire with pinning events for the notch E shallow).

There are several conclusions that can be extracted from Fig. 2. First one can see that H_{dep} , on average, increases with the notch depth, in agreement with previous results from other authors.^{9,11,13} On average, H_{dep} is around 70 Oe for deeper notches and around 40 Oe for shallower notches. The values of H_{dep} do not seem to be particularly dependent on the notch shape.⁵ For most of the notch shapes, the H_{dep} values for different wires are quite scattered, which is perhaps a bit surprising considering that all the wires for a given notch depth belong to the same sample. This stochastic behavior between wires seem to be smaller for S deep and C deep but we will come back to this later in the paper. H_{prop} is clearly close to 40 Oe in wires with deeper notches while this value is smaller for wires with shallower notches. One possibility is that being H_{dep} lower for wires with shallow notches, injection events with $H_{\text{prop}} > H_{\text{dep}}$, would be rarely detected between contacts B and C in Fig. 1. A way of checking this assumption is by detecting the DW in the curved section (contacts C and D in Fig. 1) so we measure H_{prop} in the nonpinning events. This value in the samples measured averages 20 Oe, which is still much smaller than the average H_{dep} for the sample with shallow notches. Other possibility is that this higher H_{prop} for the sample with deeper notches may be due to larger edge roughness in this sample. Nevertheless, when we compare the AFM images of both samples, we do not see any obvious difference in the edge roughness. This leaves the microstructure of the material as the only possible explanation to the difference in H_{prop} between the two samples. The microstructure of the permalloy may change due to small differences in the deposition process (small changes in substrate temperature, Ar pressure, deposition rate, etc.) and it seems to be quite critical for the detailed magnetization process of the wire.¹⁵

In order to see which type of notch perform best, we need

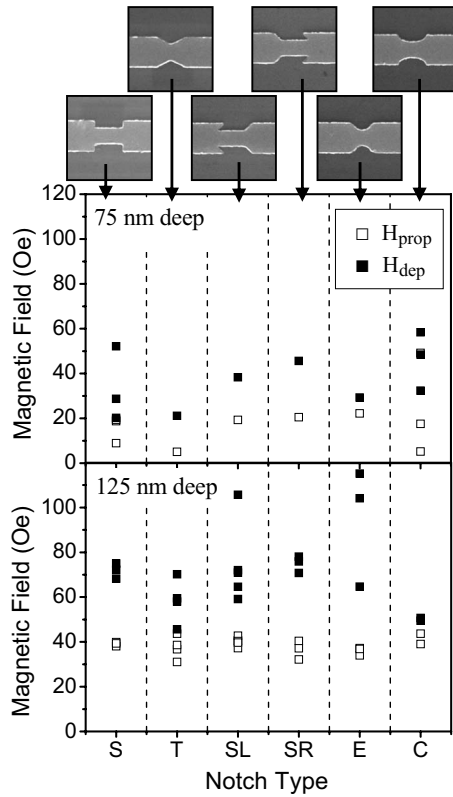


FIG. 2. Propagation field (open squares) and depinning field (solid squares) for all the wires and the notches measured in this study. Each point represents the average value of at least 40 measurements. The top graph plots the values for wires with shallow notches and the bottom graph plots the values for deeper notches. On top of the figure there are SEM pictures for each of the notches studied: S—square, T—triangular, SL—square left, SR—square right, E—elliptical, and C—circular. The width of all the wires is 500 nm.

to complete the information shown in Fig. 2 with the total probability of pinning. Figure 3 shows the probability of pinning (top graph) for every notch type and depth, taking into account all the events and all the wires measured for every type of notch. The only shape that shows probability of pinning 1 is the square for both shallow notches (127 measurements) and deep notches (110 measurements). Also SL deep (180 measurements) and E deep (120 measurements) show very good pinning probability. The triangle probability is surprisingly low when it is quite a reliable pinning shape in narrower permalloy wires.^{3,16} This could indicate that a 30% deep notch (percentage over the width of the wire) on one side of the wire might be more effective pinning center than two symmetrical 15% deep notches with the same shape.

Also in Fig. 3 (bottom graph), we represent the standard deviation of H_{dep} measured in each type of notch. When a type of notch is measured in more than one wire, we plot the average of the standard deviations for all the wires measured with that type of notch. This value gives us an idea of how scattered the values of H_{dep} are. Square notches of both depths have quite a low dispersion, also triangular and SL deep. The case of the triangle is quite interesting as the pinning probability is not very good but the pinning events are

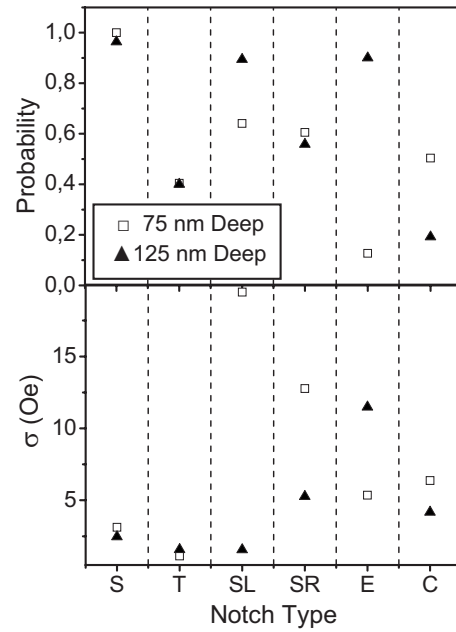


FIG. 3. Top graph represents the probability of pinning for each type of notch. Some data of the total number of measurements are given in the main text. Bottom graph represents the standard deviation for all the measurements for the different notches. Empty squares are measurements for shallow notches and solid triangles for deeper notches.

always very similar. For the E deep notch the dispersion is high due to four depinning events (out of 108 pinning events) which are largely different to the rest of the values. Removing these values out of the dispersion, we would obtain a standard deviation of about 7 Oe.

From Figs. 2 and 3 we can conclude that the square double notches are the most effective pinning centers, together with SL deep and perhaps E deep. All of them have also a relatively low dispersion in the measured H_{dep} . For practical applications, even a very small dispersion in the depinning energy might be critical, especially in memories where there can be thousands of events every second. It is very important therefore to explore the reasons behind this dispersion.

We have chosen symmetrical dual notches for this work because they should be insensitive to the chirality of the DW.⁵ Despite this, from our AMR measurements it is obvious that there are several depinning mechanisms. As an example, Fig. 4 shows the AMR signal for the DW depinning process in a S-deep notch. All the depinning events for S-deep notches follow one of the two profiles shown in Fig. 4, A or B, indicating at least two major different depinning processes (perhaps two different types of DW). The other type of notches have their own particular profiles, not necessarily similar to the ones shown in Fig. 4. This figure shows clearly that when the AMR depinning profile for different measurements is identical, the dispersion in their H_{dep} is negligible. On the other hand, if their profiles are even marginally different, the values of H_{dep} can differ significantly. This is shown clearly in the right plot of Fig. 4 where there is only a small difference between the profiles (marked with a

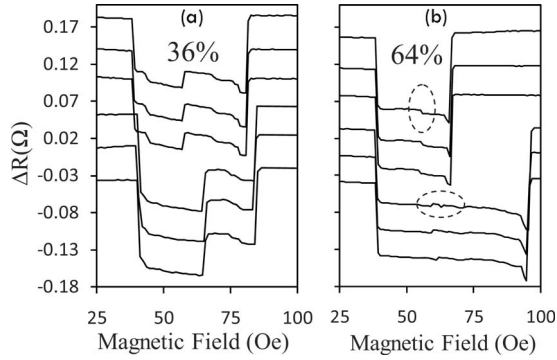


FIG. 4. Plots (a) and (b) show the two typical shapes found for the AMR profile in the pinning events measured for S-125 nm notch. The percentage of events for each type is indicated on top of the figures. For both (a) and (b) we show six events displaced for clarity. It is clear that if the profile is identical for different events (i.e., the bottom three curves), H_{dep} is the same. On the other hand, if the shape changes even marginally (compare the bottom three curves with the top three in both (a) and (b) H_{dep} can be considerably different. The dashed ellipses on the right plot indicate the only difference between the three top and three bottom curves.

dashed ellipse) but the depinning field is considerably different. A change in the AMR signal comes from a change in the transversal magnetization component (the component perpendicular to the current direction) of the DW. Therefore, this dependence of the dispersion of H_{dep} with the AMR profile suggests that even small differences in the shape of the DW at the notch can determine largely the depinning field. The exact shape of the pinned DW at the notch will depend on thermal fluctuations, interactions of the local magnetization with the nanometric landscape around the notch and on the exact H_{prop} . Note that as H_{prop} is in all our measurements quite likely over the Walker field, the traveling DW experiences constant transformations^{17,18} and the exact shape of the pinned DW would depend on the exact particular conditions on arrival to the notch. Many of the factors that condition the exact DW profile at the notch have a stochastic nature and this implies that the depinning energy will have an inherent random component.

In order to better understand the depinning process, we have performed micromagnetic simulations for all the notches used in this study. The simulations were performed using the OOMMF software package and standard permalloy parameters, $M_s = 860 \times 10^3$ A/m, exchange energy constant $A = 13 \times 10^{-12}$ J/m, and zero magnetocrystalline anisotropy. Using the well-established phase diagram of DWs in planar permalloy nanowires,¹⁹ a vortex wall (for both chiralities) was introduced at the left end of a 4- μm -long, 500-nm-wide, and 15-nm-thick permalloy nanowire, using a 5 nm mesh.

Figure 5 shows the three types of depinning processes that we have found in the simulations of the different wires and notches. The first one, on the left of Fig. 5, shows a “clean” depinning sequence, where the DW keeps its structure during the pinning and depinning processes. This type of sequence happens only in shallow notches with a “smooth” left edge (i.e., E, T, SR, and C shallow). The middle sequence of Fig. 5 shows how the vortex DW changes its chirality during the

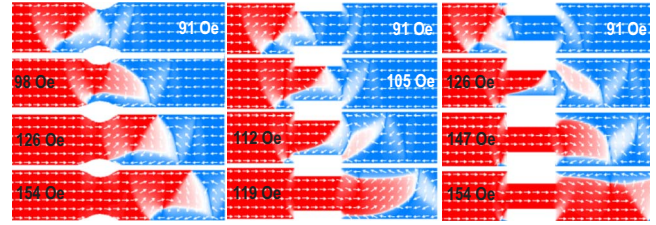


FIG. 5. (Color online) Depinning sequences in different types of notches. The left sequence describes a clean depinning in a E-shallow notch where the structure of the DW is not altered in the process. In the middle sequence for a S-shallow notch, the vortex changes chirality during the depinning. Finally, in the right sequence for a S-deep notch, a different vortex nucleates on the right of the notch before the incoming DW is extinguished on the left side of the notch.

depinning. This cannot be considered as a renucleation at the notch because after the depinning there is not a DW remaining on the left-hand side of the notch. This change in vortex chirality happens for most notches (S, SL shallow and T, SL, and SR deep). Finally, the sequence on the right of Fig. 5 shows the nucleation of a DW on the right-hand side of the notch and in the last frame a pinned vortex on the bottom left side of the notch coexist with the newly nucleated DW exiting the right side of the notch. This double nucleation in deep notches has been suggested before⁹ and it occurs in S- and C-deep notches. In Fig. 5, it is also interesting to note how in the middle and in the right sequences, the DW gets highly stretched before depinning totally. It seems like the shape of the exiting side of the notch is the one determining H_{dep} for most types of notches²⁰ (for those with sharp edges of dimensions comparable to the DW width).

The simulations shows that, although S-deep notches are very effective pinning centers and with low dispersion in the values of H_{dep} , the depinning process is achieved only via double nucleation which is not ideal for any application. Taking into account the simulations, the probability of pinning and the dispersion in the measurements, the best double notches are S shallow and E deep (although its depth should perhaps be slightly smaller in order to avoid the change in vortex polarity during the depinning process).

In this work we have performed a study of the pinning process of a DW for different shapes of the notch. Taking into account the probability of pinning, the dispersion of the measured H_{dep} and the simulated depinning process, it seems that two of the shapes are more effective than the rest (S shallow and E deep). Beyond the performance of a particular notch as a pinning center, we observe a dispersion in the values of H_{dep} which seems to be unavoidable for any shape. Dispersion in the depinning measurements is also present in all previous works that show more than one measurement for a given structure.

The precise AMR profile of the DW measured during the pinning process showed that the dispersion in the values of H_{dep} comes together with variations in that AMR profile. Those variations are necessarily associated with changes in the profile of the pinned DW. The exact microstructure of the pinned DW in the vicinity of the notch depends not only on the geometry or quality of the patterned notch, but also on

the structure of the moving DW approaching the notch, which depends itself on the applied field (or polarized current). The speed of the moving DW is also subject of dispersion,²¹ depending on the energy supplied to the system, which of course would affect the exact profile of the DW when it arrives to the notch. Therefore it seems that the pinning potential has an intrinsic random component which can be very negative for practical applications. Working with narrower wires would be better in terms of reducing the possible DW configurations. On the other hand, for very narrow wires, making a reproducible patterning of notches is very challenging with present lithography techniques. Therefore, in order to make the pinning of a DW reliable and reproducible, we ought to explore other type of defects, perhaps struc-

tural, where the magnetic profile of the pinned DW is forced by the defect itself or even different materials rather than permalloy.

Additionally, works that rely on the depinning of a DW from a notch in order to calculate some intrinsic parameters of the material (e.g., spin transfer torque), ought to be very careful drawing conclusions from the measurements of a single wire, unless the experimental results are accompanied with careful simulations.

We acknowledge the Spanish Ministerio de Ciencia e Innovación for funding this work through Grants No. MAT2008-02770/NAN and No. MAT2009-08771.

-
- ¹J. C. Slonczewski, *J. Magn. Magn. Mater.* **159**, L1 (1996).
²S. S. P. Parkin, U.S. Patent No. 6,834,005 (2004).
³S. S. P. Parkin, M. Hayashi, and L. Thomas, *Science* **320**, 190 (2008).
⁴M. Hayashi, L. Thomas, C. Rettner, R. Moriya, and S. S. P. Parkin, *Appl. Phys. Lett.* **92**, 162503 (2008).
⁵L. K. Bogart, D. Atkinson, K. O'Shea, D. McGrouther, and S. McVitie, *Phys. Rev. B* **79**, 054414 (2009).
⁶D. Petit, A. Jausovec, D. Read, and R. Cowburn, *J. Appl. Phys.* **103**, 114307 (2008).
⁷K. He, D. Smith, and M. R. McCartney, *Appl. Phys. Lett.* **95**, 182507 (2009).
⁸C. C. Faulkner, M. D. Cooke, D. A. Allwood, D. Petit, D. Atkinson, and R. P. Cowburn, *J. Appl. Phys.* **95**, 6717 (2004).
⁹L. K. Bogart, D. S. Eastwood, and D. Atkinson, *J. Appl. Phys.* **104**, 033904 (2008).
¹⁰M. Herrmann, S. McVitie, and J. N. Chapman, *J. Appl. Phys.* **87**, 2994 (2000).
¹¹A. Himeno, S. Kasai, and T. Ono, *J. Appl. Phys.* **99**, 08G304 (2006).
¹²M. Hayashi, Ph.D. thesis, Stanford University, 2006.
¹³M.-Y. Im, L. Bocklage, P. Fisher, and G. Meier, *Phys. Rev. Lett.* **102**, 147204 (2009).
¹⁴R. Lavrijsen, J. H. Franken, J. T. Kohlhepp, H. J. M. Swagten, and B. Koopmans, *Appl. Phys. Lett.* **96**, 222502 (2010).
¹⁵G. Nahrwold, J. M. Scholtyssek, S. Motl-Ziegler, O. Albrecht, U. Merkt, and G. Meier, *J. Appl. Phys.* **108**, 013907 (2010).
¹⁶We are conducting other nonrelated experiments on permalloy wires 300 nm wide and 10 nm thick, with a 30% deep triangular notch on one side of the wire and we find that the pinning probability in some field range is always 1, over many different wires and many different samples. Note that a pinning probability 1 does not give any information about the dispersion on the values of H_{dep} , which is the subject of this work.
¹⁷M. Hayashi, L. Thomas, C. Rettner, R. Moriya, and S. S. P. Parkin, *Nat. Phys.* **3**, 21 (2007).
¹⁸J. Y. Lee, K. S. Lee, S. Choi, K. Y. Guslienko, and S. K. Kim, *Phys. Rev. B* **76**, 184408 (2007).
¹⁹Y. Nakatani, A. Thiaville, and J. Miltat, *J. Magn. Magn. Mater.* **290-291**, 750 (2005).
²⁰S. B. Choe, *J. Magn. Magn. Mater.* **320**, 1112 (2008).
²¹X. Jiang, L. Thomas, R. Moriya, M. Hayashi, B. Bergman, C. Rettner, and S. S. P. Parkin, *Nat. Comput.* **1**, 25 (2010).